THE JOURNAL OF BIOLOGICAL CHEMISTRY VOL. 283, NO. 37, pp. 25218–25226, September 12, 2008

The Thermodynamics and Kinetics of Electron Transfer between Cytochrome b_6f and Photosystem I in the Chlorophyll *d*-dominated Cyanobacterium, *Acaryochloris marina**

Received for publication, April 21, 2008, and in revised form, July 16, 2008 Published, JBC Papers in Press, July 16, 2008, DOI 10.1074/jbc.M803047200

Benjamin Bailleul[‡], **Xenie Johnson**[‡], **Giovanni Finazzi**[‡], **James Barber**[§], **Fabrice Rappaport**[‡1], **and Alison Telfer**[§2]

From the [‡]*Institut de Biologie Physico-Chimique, UMR 7141 CNRS-Université Paris 6, 13 Rue Pierre et Marie Curie, Paris 75005, France and the* [§]*Division of Molecular Biosciences, Imperial College London, Biochemistry Building, South Kensington Campus, London SW7 2AZ, United Kingdom*

We have investigated the photosynthetic properties of *Acaryochloris marina*, a cyanobacterium distinguished by having a high level of chlorophyll *d*, which has its absorption bands shifted to the red when compared with chlorophyll *a*. Despite this unusual pigment content, the overall rate and thermodynamics of the photosynthetic electron flow are similar to those of chlorophyll *a*-containing species. The midpoint potential of both cytochrome *f* and the primary electron donor of photosystem I (P_{740}) were found to be unchanged with respect to those prevailing in organisms having chlorophyll *a*, being 345 and 425 mV, respectively. Thus, contrary to previous reports (Hu, Q., Miyashita, H., Iwasaki, I. I., Kurano, N., Miyachi, S., Iwaki, M., and Itoh, S. (1998) *Proc. Natl. Acad. Sci. U. S. A.* 95, 13319–13323), the midpoint potential of the electron donor P_{740} has not been tuned to compensate for the decrease in excitonic energy in *A. marina* and to maintain the reducing power of photosystem I. We argue that this is a weaker constraint on the engineering of the oxygenic photosynthetic electron transfer chain than preserving the driving force for plastoquinol oxidation by P_{740}, via the cytochrome b_6f complex. We further show that there is no restriction in the diffusion of the soluble electron carrier between cytochrome b_6f and photosystem I in *A. marina*, at variance with plants. This difference probably reflects the simplified ultrastructure of the thylakoids of this organism, where no segregation into grana and stroma lamellae is observed. Nevertheless, chlorophyll fluorescence measurements suggest that there is energy transfer between adjacent photosystem II complexes but not from photosystem II to photosystem I, indicating spatial separation between the two photosystems.

Acaryochloris marina is an unusual cyanobacterium, because it contains mainly chlorophyll (Chl)[3] *d*. It was first isolated from a suspension of algae squeezed out of *Lissoclinum patella*, a colonial ascidian (1). It mainly grows as a biofilm on the undersurface of the ascidian beneath a symbiotic layer of a *Prochloron*, which is in the upper tunic of the ascidian (2). Other varieties of *Acaryochloris* have been found on the underside of the thallus of red algae (3) and free living in a salt lake (4). The general feature of its habitat is that it lives at relatively low light intensities, which are enriched in the far red region of the spectrum. Therefore, its oxygenic photosynthesis provides a typical example of adaptation to specific light conditions (2), as evidenced by its pigment composition, where Chl *d* is predominant and the Chl *a* level is very low (5, 6). This pigment composition contrasts with the usual high level of Chl *a* found in other oxygenic phototrophes, as illustrated by the absorption spectrum of a suspension of *A. marina* cells, which is markedly red-shifted when compared with other Chl *a*-containing photosynthetic organisms. The extent of the red shift of the absorption spectrum of *A. marina* is of similar magnitude to that observed between Chl *d* and *a* in organic solvent (*e.g.* methanol) (7).

Not surprisingly, the unusual absorption spectrum of *A. marina*, due to the high level of Chl *d*, influences the spectroscopic signatures of the various cofactors involved in the primary photochemistry. For example, light-induced charge separation in photosystem I (PSI) is associated with a main absorption band (in the Qy region) bleaching maximally at 740 nm, indicating that the primary donor is composed of Chl *d* rather than Chl *a*. Hence, this pigment was named P_{740} (8). Clearly, the energy of the quantum inducing charge separation by P_{740} is lower than that of P_{700} present in Chl *a* containing PSI (1.68 eV instead of 1.77 eV). This decrease by about 100 meV is significant when compared with the ~800 meV required to drive electron transfer between the soluble electron donor to P_{740}^+ (plastocyanin) and the first soluble electron acceptor (ferredoxin). However, some specific strategies may have been developed by this organism to cope with this peculiar situation and maintain a photosynthetic activity compatible with its

* This work was supported by the Biotechnology and Biological Science Research Council, United Kingdom, and by CNRS and Université Pierre et marie Curie, Paris 6. The costs of publication of this article were defrayed in part by the payment of page charges. This article must therefore be hereby marked "*advertisement*" in accordance with 18 U.S.C. Section 1734 solely to indicate this fact.

[1] To whom correspondence may be addressed. Tel.: 33-1-5841-5059; E-mail: Fabrice.Rappaport@ibpc.fr.

[2] To whom correspondence may be addressed. Tel.: 44-20-759-41774; E-mail: a.telfer@imperial.ac.uk.

[3] The abbreviations used are: Chl, chlorophyll; cyt, cytochrome; DCMU, 3-(3,4-dichlorophenyl)-1,1-dimethylurea; DBMIB, 2,5-dibromo-3-methyl-6-isopropyl-*p*-benzoquinone; P_{700} and P_{740}, chlorophyll dimer bearing the long-lived cation in photosystem I in Chl *a* and Chl *d* organisms, respectively; PC, plastocyanin; PSI and PSII, photosystem I and II, respectively; RP, radical pair; MK, menaquinone; PQ, plastoquinone; MES, 4-morpholineethanesulfonic acid.

growth requirements. A possible rationale came from the study by Hu *et al.* (8), who measured the midpoint potential of P_{740} and found that it was down-shifted by about 100 mV when compared with that of P_{700}, the primary electron donor in PSI, where only Chl *a* is present. On this basis, they suggested that the lower midpoint potential of P_{740} would compensate for the lower energy of the absorbed quantum, thereby maintaining the reducing power of the excited state. Although such a tuning of the midpoint potential of P_{740} would allow a similar energetic picture for the electron acceptor side of PSI in *A. marina* and in Chl *a*-containing species, it would result in a significant thermodynamic pitfall on the donor side of PSI by decreasing the free energy gap between P^+_{740} and its electron donors. For example, the midpoint potential of cytochrome (cyt) *f*, in Chl *a*-containing organisms is in the 320–370 mV range (9–11). If cyt *f* in *A. marina* has the same midpoint potential, the driving force for electron transfer between cyt *f* and P^+_{740} would be slightly uphill. This would lead to the accumulation of a significant fraction of P^+_{740} under steady state illumination, which would obviously reduce the overall photochemical efficiency by closing most of the PSI photochemical traps. Alternatively, the midpoint potential of the redox-active cofactors involved in electron donation supply to P^+_{740} (the Rieske FeS center, cytochrome *f*, and plastocyanin or cyt c_6) would have to be tuned to compensate for the loss in oxidizing power of P_{740} so as to provide a driving force for maintaining efficient electron flux through PSI.

These issues are addressed in the present work. We first determined the thermodynamic equilibrium constant of the electron transfer reaction between cyt *f* and P_{740} in actively growing cells. The equilibrium constant for this reaction was found to be ~15, showing that the midpoint potential of cyt *f* is about 70 mV lower than that of the P^+_{740}/P_{740} couple. Consistent with this, the directly measured midpoint potentials of cyt *f* and of the P^+_{740}/P_{740} couples were 345 and 425 mV, respectively, in contradiction of the previous report by Hu *et al.* (8) of a midpoint potential of 335 mV for the latter. The values that we have determined are similar to those found for the analogous redox cofactors in Chl *a* organisms for cytochrome b_6f (9–11) and P_{700} (12, 13), suggesting that the midpoint potential of the primary electron donor in PSI is not necessarily affected by the chemical nature of the Chls that comprise it. This finding raises interesting questions concerning the overall energetics of PSI-driven charge separation in *A. marina*, which are discussed in this paper.

EXPERIMENTAL PROCEDURES

Growth Conditions—*A. marina* cells were grown under low white light illumination (5–10 microeinsteins m^{-2} s^{-1}) in a modified K^+ESM medium (14, 15) supplemented with extra iron to a final concentration of 14 μM. The cyanobacterium was harvested in its midexponential phase, and the cells were resuspended in fresh medium at the desired density for experiments.

Membrane Isolation—Thylakoid membranes were prepared from freshly harvested cells, which were resuspended in a medium containing 50 mM MES, pH 6.5, 20–25% glycerol (W/v), 10 mM $CaCl_2$, 5 mM $MgCl_2$, and 1 mM benzamidine. Cells were broken by several cycles of centrifugation in the presence of 0.1-mm glass beads (10 s), followed by a short (10 s) incubation in an ice bath. Unbroken cells were removed by a short centrifugation at 2000 × *g*. Thylakoid membranes were recovered from the supernatant, after an additional centrifugation at 80,000 × *g* for 30 min. The final pellet was resuspended in a 50 mM MES, pH 6.5, buffer, in the presence of 20 mM $CaCl_2$ and 2.5 mM $MgCl_2$.

RNA Isolation and Reverse Transcription-PCR—RNA was isolated using a hot phenol acid method for *Synechocystis* sp. PCC 6803[4] adapted from Ref. 16. Total RNA was treated with 1 unit/μg RNA for 1 h with DNase (Promega). 350 ng of total RNA was used in a reverse transcription reaction according to the manufacturer's instructions (BcaBEST RNA PCR kit version 1.1; TaKaRa), using a specific reverse primer (5′-TTAGCCCTGAACCGTAATGG-3′) to the *petE* genomic DNA sequence (accession number: YP_001517679), and the entire volume was added to the subsequent PCR (94 °C 30 s, 57 °C 30 s, 72 °C 1 min for 35 cycles) using a specific forward primer (5′-TCAAATGGGGTCTTCTACGG-3′).

Spectroscopy—Absorption and fluorescence spectra were measured with a laboratory-built spectrophotometer based on a diode array (AVS-USB 200; Ocean Optics). Excitation of fluorescence was at 470 nm unless otherwise indicated. Spectroscopic analysis was performed at room temperature, using home-made pump and probe spectrophotometers. Three different set-ups were employed. The kinetics of light-induced redox changes were measured with a LED-based spectrophotometer (JTS10, Biologic, France), having a time resolution of 10 μs (Figs. 2 and 5). Actinic flashes were provided by a dye laser at 690 nm, whereas measuring flashes were provided by a white LED (Luxeon; Lumileds) fitted with appropriate interference filters (10 nm full width at half-maximum). Alternatively, a second set-up having a time resolution of 10 ns (17) was employed, in which the actinic flashes were provided by a dye laser at 690 nm, whereas probe flashes were generated by an optical parametric oscillator pumped by an Nd:Yag laser (Figs. 3 and 4). The third set-up was for electrochemical redox titrations, which were measured as described previously (18, 19) (Fig. 6). In this case, the actinic flashes were provided by a xenon flash lamp (giving saturating light pulses, 5-μs duration at half-height), passed through a Schott RG695 interference filter. Probe flashes were provided by a second xenon flash lamp (3-μs duration at half-height), filtered through a monochromator (Jobin Yvon). Titration of cyt *f* was performed measuring the absorption changes at 554 nm, with a base line drawn between 546 and 562 nm. Mediators were *para*-benzoquinone, diaminodurene, 2,5 dimethyl-benzoquinone, phenazine methosulfate, and menadione, at a concentration of 1 μM for each. Similarly, the redox potential of P_{740} was measured using the amplitude of the flash-induced absorption changes (at 740 nm) at various redox potentials, poised either electrochemically or chemically.

RESULTS

Absorption and Fluorescence Emission Spectra—Cells of *A. marina*, in midexponential phase, were used to characterize the main properties of the intersystem electron transport chain in

[4] G. Ajlani, personal communication.

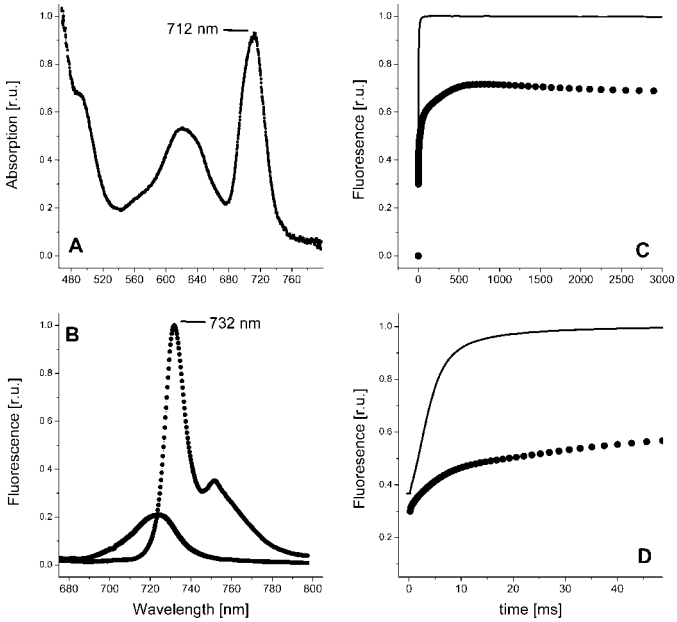

FIGURE 1. *A* and *B*, absorption spectrum (*A*) at room temperature and fluorescence spectra (*B*) at room temperature (*solid line*) and 77 K (*dotted line*) of a suspension of *A. marina* cells. Room temperature fluorescence induction kinetics (*C* and *D*, on an expanded scale) was measured in the presence (*solid line*) and absence (*dotted line*) of the PSII inhibitor DCMU. Cells were harvested in midexponential phase and resuspended in fresh growth medium before measurements. See "Experimental Procedures" for further experimental details.

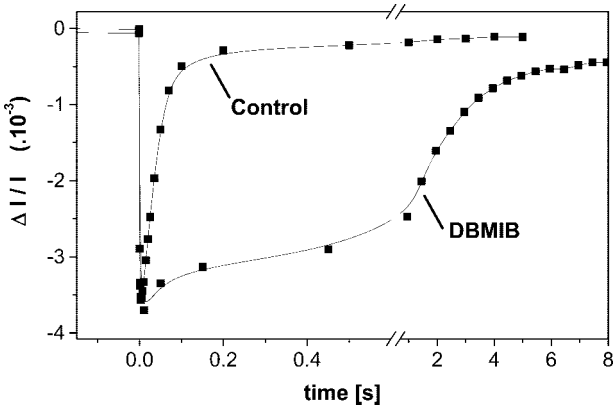

FIGURE 2. **Light-induced absorption changes at 554 nm.** Absorption changes associated with the redox changes of the cytochromes were measured after a saturating illumination in the absence and presence of DBMIB (5 μM).

this cyanobacterium. Fig. 1, *A* and *B*, shows their absorption and fluorescence spectra, respectively. The room temperature absorption spectrum is characterized by a major peak at ~712 nm, consistent with the pigment content of this organism, where Chl *d* is predominant (1). A second broad peak is seen in the 600–650 nm range, consistent with the presence of significant amounts of phycobiliproteins, which together with Chl *d*-binding Pcb proteins, provide a light harvesting system to *Acaryochloris* (5, 20, 21). The fluorescence emission spectra show a main peak at 724 nm at room temperature, which is shifted to 732 nm at 77 K. No significant emission from the phycobiliproteins or from detached Pcb proteins is seen, either under the conditions shown (chlorophyll-selected excitation at 470 nm; Fig. 1*B*) or after specific excitation of the phycobilins at 590 nm (data not shown). Thus, all of the light harvesting complexes are tightly coupled to the photochemical traps, in agreement with previous reports (22).

Overall Photosynthetic Activity—The overall photosynthetic activity of *A. marina* was evaluated from the fluorescence induction curve shown in Fig. 1, *C* and *D*. The quantum yield of PSII, $F_v/F_m = ((F_m - F_o)/F_m)$ (23–25) gave a typical value of ~0.7 for F_v/F_m, which is in agreement with previous reports (20). This is higher than values for other phycobilisome-containing cyanobacteria (see Ref. 26) for a review). In these organisms, the low F_v/F_m ratio is interpreted as reflecting either the presence of sustained energy spillover from PSII to PSI (27), the loose excitonic connectivity between the phycobilisomes, or the photochemical traps (which is not the case here; see above), or the low PSII/PSI ratio (reviewed in Ref. 26)). Neither of these phenomena significantly occur in *A. marina*, since the large F_v/F_m is incompatible with a low amount of PSII, and the shape of the fluorescence rise, measured in the presence of the PSII inhibitor, 3-(3,4-dichlorophenyl)-1,1-dimethylurea (DCMU), is clearly sigmoidal (Fig. 1*C*) (also see Ref. 20). This feature, which is commonly observed in photosynthetic eukaryotes but not in cyanobacteria, is interpreted as reflecting the progressive increase in the light harvesting capacity of a PSII photochemical unit as its PSII neighbors become photochemically inactive due to the reduction of the quinone acceptor Q_A (28, 29). Such a feature is indicative of efficient energy transfer between closed and open PSII traps, without any significant competition by energy quenching through PSI photochemistry.

Another important feature of the fluorescence data shown in Fig. 1 is the large difference between the level measured under steady state (F_s), noninhibited conditions (control in Fig. 1*D*) and the maximum level (F_m) (+*DCMU* in Fig. 1*D*). Since F_s is expected to reflect the steady state amount of reduced Q_A, this finding suggests that the limiting step in the reoxidation of the plastoquinone pool (*i.e.* in the electron flow downstream of PSII) is in the same range as the rate of its reduction (*i.e.* the number of electrons transferred by PSII per unit of time). As discussed by Joliot (28, 30), this can be empirically estimated from the time required to reach ~66% of the F_m value, in the presence of DCMU. Since this value is ~10 ms in the present experiment (Fig. 1*D*), it can be deduced that the number of electrons transferred per photosynthetic chain is in the 100 s^{-1} range (*i.e.* close to the maximum rate of PQH_2 oxidation *in vivo*) (31). In other words, there seems to be no severe bottleneck in electron transfer downstream of PSII in *A. marina.*

Kinetic Features of the Electron Flow Chain—Following on from above, we investigated further the properties of the electron transfer chain by directly measuring the photochemically induced turnover of the cytochrome b_6f complex. Fig. 2 shows the time course of the changes occurring at 554 nm upon excitation with a single turnover saturating flash. At this wavelength, the actinic flash induces a rapid bleaching (see Fig. 2). The recovery kinetics, to the initial (dark-adapted) level, was inhibited by addition of the plastoquinone analogue, 2,5-dibromo-3-methyl-6-isopropyl-p-benzoquinone (DBMIB) (32), as expected if it reflects electron flow from PSII through the lumenal (Q_0) site of the cytochrome b_6f complex.

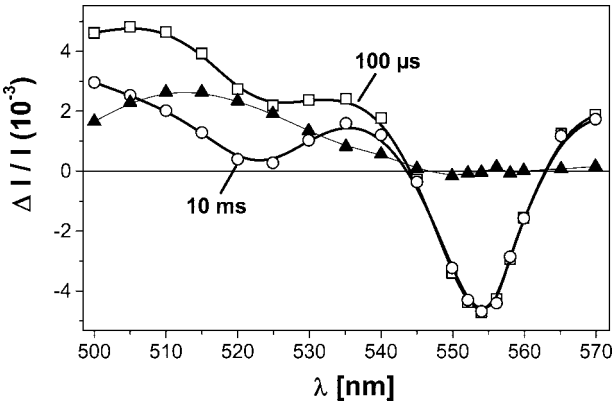

FIGURE 3. **Light-induced absorption changes between 500 and 570 nm.** DBMIB (5 μM) was added to slow down signal recovery between each flash and allow integration of the absorption signal. Absorption was measured 100 μs and 10 ms after the last flash. The rather featureless difference between those two spectra (*triangles*) is attributed to electrochromic bandshift.

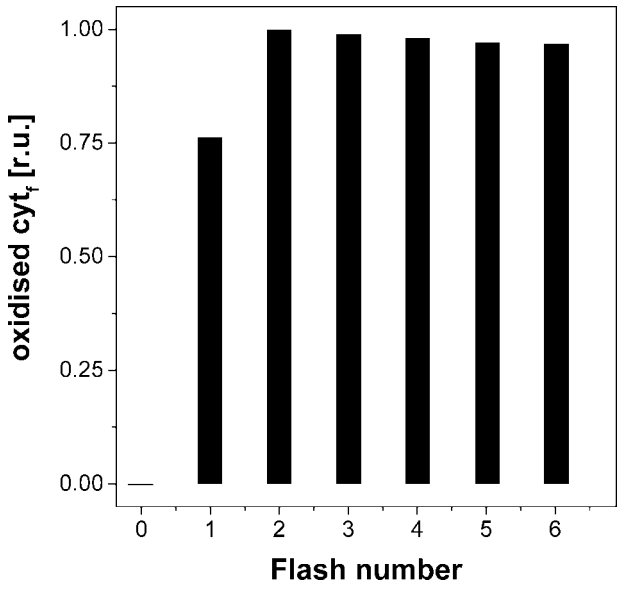

FIGURE 4. **Relative amplitude of the signal at 554 nm, measured 10 ms after a saturating flash as a function of the number of actinic flashes during a series of 10 closely spaced (150 ms) saturating pulses.** Conditions were the same as in Fig. 3. DBMIB was present at a concentration of 5 μM.

Fig. 3 shows two spectra measured 100 μs and 10 ms after the last flash of a series of 10. Both spectra show pronounced bleach at 554 nm and a less pronounced one around 520 nm. Conversely, the absorption changes comprised between 100 μs and 100 ms (see difference spectrum in Fig. 3) were rather featureless, with a broad absorption increase peaking at 515 nm. The two bleaching bands, at 554 and 520 nm, are characteristic of the oxidation spectrum of *c*-type cytochrome (they correspond to the α and β bands of the reduced state, respectively; see Ref. 33). We tentatively ascribe the broad absorption change at 515 nm to an electrochromic band shift undergone by pigments embedded in the membrane upon generation of a transmembrane electric field due to PSI and PSII photochemical activity (34). Interestingly, no absorption changes were observed at 554 nm between 100 μs and 10 ms, suggesting that there is no contribution of the electrochromic band shift at this wavelength, indicating that this wavelength may be used with confidence to follow the redox changes of *c*-type cytochromes.

The observation of a light-induced oxidation of one or more *c*-type cytochrome(s) raises the question of the identity of these oxidized redox carriers. The absorption changes shown in Figs. 2 and 3 can be taken as the signature of the oxidation of either cyt *f* alone or with a soluble cyt c_6. The latter is known to act as a soluble electron carrier between the cyt b_6f complex and PSI in some cyanobacteria (35) (see Ref. 36 for a review), and it cannot be ruled out as an electron carrier in *A. marina*, where two putative genes coding for cyt c_6 are present in the genome sequence (37). On the other hand, a gene encoding for plastocyanin is also found in this cyanobacterium (37).

To determine the nature of the soluble electron carrier between the cyt b_6f complex and PSI, we measured the progressive increase in the absorption changes associated with the *c*-type cytochrome oxidation, at 554 nm, during a series of 10 flashes (Fig. 4). Again, DBMIB was added to prevent the rereduction of the cytochromes by plastoquinol (32). As shown in Fig. 4, about 75% of the absorption changes were observed after the first flash in the series. This shows that a single charge separation at the level of PSI is sufficient to oxidize 75% of the *c*-type cytochrome. Thus, the pool of electron donor to P_{740}^+ which gives rise to an absorption change at 554 nm is not in excess with respect to the PSI content. Since the soluble electron carriers, such as cyt c_6 or plastocyanin, are usually found in an ~3:1 ratio with respect to PSI (see Ref. 36 for a review), we ascribe the 554 nm bleaching to cyt *f* and propose that plastocyanin, the redox changes of which are not associated with any significant absorption changes in this wavelength region, mediates electron transfer between PSI and the cyt b_6f complex.

Ideally, this proposal should be backed up by the direct observation of absorption changes associated with plastocyanin redox changes. However, in the case of *A. marina*, the red-shifted oxidation spectrum of P_{740} (8, 38, 39) strongly overlaps with the oxidation spectrum of plastocyanin (the redox changes of which are commonly followed in the 810–870 nm region), making the direct observation of plastocyanin redox changes using optical spectroscopy difficult.

To circumvent this, reverse transcription-PCR was performed on total RNA samples from *A. marina* to test expression of the *petE* gene hypothetically coding for plastocyanin. We observed a band of the expected size (285 nt) when reverse transcriptase was added to the reaction and no product in the negative control (Fig. 5), suggesting that the *petE* gene is expressed under the present conditions and providing support for the presence of plastocyanin as a soluble carrier under these conditions. Similar experiments aimed at testing the expression of the two *petJ* genes hypothetically coding for cytochrome c_6 proved inconclusive (data not shown). Thus, cytochrome c_6 cannot be strictly ruled out, but it would have to be present in largely substoichiometric amounts with respect to PSI to account for the fact that 75% of the absorption changes resulting from the complete oxidation of the cytochrome pool are obtained after the injection of a single oxidizing equivalent in the chain, as shown in Fig. 4.

Redox Equilibration within the Electron Transfer Chain—The fact that 75% of the oxidizing equivalents generated by PSI eventually end up on cyt *f* in itself suggests that the equilibrium

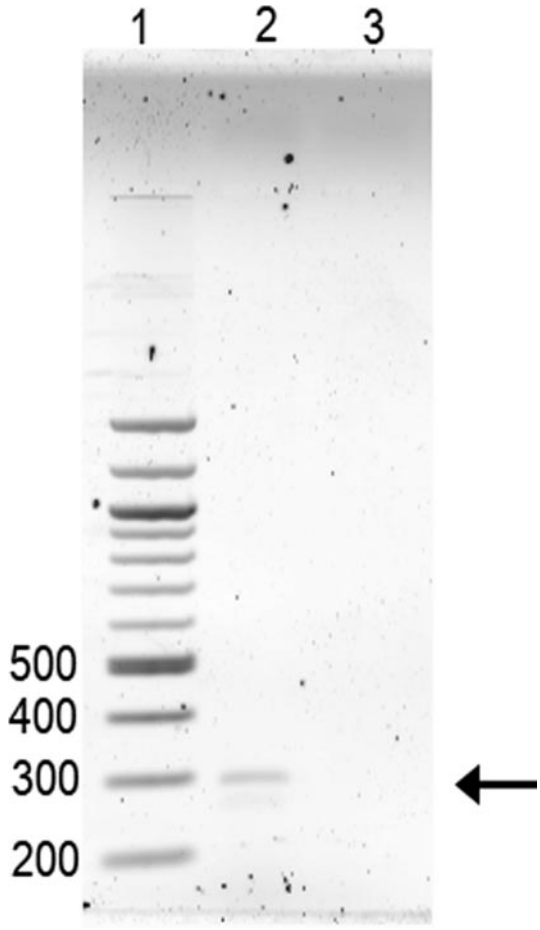

FIGURE 5. **RT-PCR on total RNA isolated from *A. marina* to amplify the *petE* gene.** *Lane 1*, 100-bp ladder. *Lane 2*, RT-PCR using petE-specific primers. *Lane 3*, no reverse transcriptase added to reaction as negative control. Samples were migrated for 1 h on a 1.4% agarose gel.

constant of the electron transfer reaction between these two redox cofactors is larger than one. This is at odds with the expectation that could be drawn from the difference in midpoint potential between the P^+_{740}/P_{740} and cyt f^{ox}/cyt f couples based on the results of Hu *et al.* (8).

By definition, the equilibrium constant K_{fp} between the P^+_{740}/P_{740} and cyt f^{ox}/cyt f couples is as follows,

$$K_{fp} = \frac{[\text{cyt } f^{ox}][P_{740}]}{[\text{cyt } f][P^{ox}_{740}]} \qquad \text{(Eq. 1)}$$

where [cyt f], [cyt f^{ox}], [P_{740}], and [P^{ox}_{740}] represent the concentration, at equilibrium, of the oxidized and reduced form of cyt f and P_{740}. Thus, the equilibrium constant may be experimentally determined by assessing the relative amount of P^{ox}_{740} for a given value of the relative amount of cyt f^{ox}. To do so, we measured the slow rereduction in the dark of both P^{ox}_{740} and cyt f^{ox} (generated by continuous illumination beforehand). As shown in Fig. 6, this illumination regime, in the presence of DBMIB, leads to the full oxidation of both cofactors. When the actinic light is switched off, they are slowly rereduced and return to their dark-adapted redox state within the second time range. Since this is more than 4 orders of magnitude slower than the overall electron transfer between P^+_{740} and cyt f (the latter is

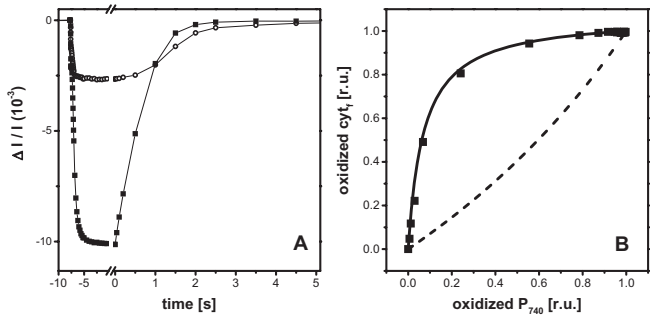

FIGURE 6. *A*, *in vivo* measurements of P_{740} and cyt f oxidation under continuous illumination and consecutive rereduction. DBMIB (5 μM) was added to slow down reduction of both cytochrome f^+ and P^+_{740}, in order to allow full equilibration between the redox partners. See "Results" for further explanation. *Open circles*, cyt f^+; *open squares*, P^+_{740}. *B*, equilibrium plots for the components of the high potential chain in *A marina*. Relaxation signals after the continuous light (see *A*) of cytochrome *f* and P_{740} were normalized and plotted against each other (*squares*). Maximum amplitudes of redox changes, at $t = 0$, were set to 1. The two curves were fitted using Equations 2–4 (*solid line*) and the simulation (*dashed line*) corresponding to a redox potential of 335 mV for P_{740} (8) and 345 mV for cyt *f* (our measurement).

oxidized in the hundreds of microseconds time range; see Fig. 3), it can be reasonably assumed that the slow rereduction of both components occurs at equilibrium. Consequently, the relative amounts of oxidized cyt *f* and P_{740} at a given time can be derived from the kinetics shown in Fig. 6*A* and plotted one against the other, as shown in Fig. 6*B*. Qualitatively, it can be seen that the reduction of cyt *f* is significantly slower than that of P^+_{740}, indicating that when an electron is reinjected into the PSI donors chain, the probability that it reduces P^+_{740} rather than cyt f^{ox} is $\gg 1$, consistent with the above conclusion that K_{fp} is larger than 1.

From Equation 1, the following relationship between the relative amount of oxidized P_{740} and of cyt *f* can be derived.

$$y = \frac{K_{fp} \cdot x}{1 + x \cdot (K_{fp} - 1)} \qquad \text{(Eq. 2)}$$

with

$$y = \frac{\text{cyt } f^{ox}}{\text{cyt } f + \text{cyt } f^{ox}} \qquad \text{(Eq. 3)}$$

and

$$x = \frac{P^{ox}_{740}}{P^{ox}_{740} + P_{740}} \qquad \text{(Eq. 4)}$$

As shown in Fig. 6, the data could be satisfyingly fitted with this function, and the fit yielded $K_{fp} = 15 \pm 1$, leading to a difference between the midpoint potentials of the P^+_{740}/P_{740} and cyt f^{ox}/cyt *f* couples of ~70 mV. Taking a value of 345 mV for the latter (9–11) and 335 mV for the former (8), the expected equilibrium constant would be ~0.8 (see *dashed line* in Fig. 6). Conversely, the value estimated by Hu *et al.* (8) for the P^+_{740}/P_{740} midpoint potential combined with $K_{fp} = 15$ would lead to a midpoint potential for the cyt f^{ox}/cyt *f* couple of ~265 mV (*i.e.* downshifted by about 100 mV with respect to Chl *a*-containing organisms). Although such a variation in the midpoint potential of a given cofactor would not be unprecedented, as illustrated by the down-shifted midpoint potential of the cytochrome b_H

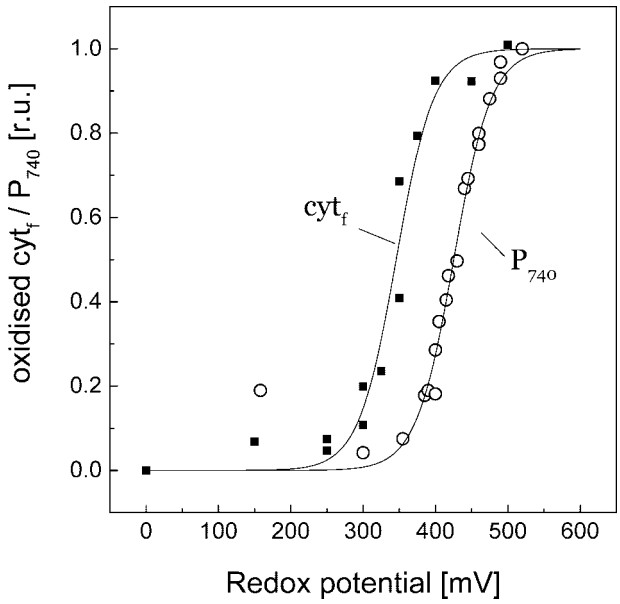

FIGURE 7. **Redox titrations in thylakoid membranes of *A marina*.** Cytochrome *f* redox state (*squares*) was measured at 554 nm. P_{740} (*circles*) was evaluated as the fraction of photo-oxidizable pigment at different redox potentials. The maximum amplitude of P_{740} and cyt *f* redox changes was arbitrarily set to 1 to allow for comparison of the different experiments.

and b_L in *Heliobacter mobilis* (40), the rather large amplitude of the putative down-shift calls for a direct measure of the midpoint potential of both redox cofactors. This is shown in Fig. 7, which presents the equilibrium redox titrations of both cyt *f* and P_{740}. For both cofactors, the data could be fitted with an $n = 1$ Nernst curve yielding E_m (cyt f^+/cyt f) = 345 ± 20 mV and E_m (P^+_{740}/P_{740}) = 425 ± 10 mV.

It is of note that the difference between these two midpoints is about 80 mV, in good agreement with our estimate above of 70 mV. However, clearly this is not consistent with the estimate of a midpoint potential of 335 mV for the P^+_{740}/P_{740} couple previously reported by Hu *et al.* (8). We therefore repeated the equilibrium redox titration by chemical (the method of Hu *et al.* (8)) rather than electrochemical titration. Similar results, within the experimental error (not shown), were obtained using both of the methods. Also, the revised midpoint potential found here for the P^+_{740}/P_{740} couple agrees with the data of Schenderlein *et al.* (41) and Tomo *et al.* (42).

DISCUSSION

Energetics of PS1 in A. marina—Our analyses of the kinetics and thermodynamic properties of the electron flow chain in *A. marina* reveals a scenario that is very similar to that found in Chl *a*-containing organisms. Indeed, despite the large displacement in the overall absorption spectrum, resulting in an overall decrease in the energy content of the photons absorbed by both PSI and PSII, photosynthetic electron flow takes place very efficiently in this cyanobacterium, where the rate of the intersystem electron flow can exceed 100 s^{-1}. Our analyses provides a rationale for such an efficient electron flow by showing that the redox potentials of both P_{740} (the primary donor of PSI) and cyt *f* are similar to those previously measured in other types of cyanobacteria, green algae, and vascular plants. Thus, the driving force for cyt *f* oxidation is very similar in both Chl *a*- and Chl *d*-based organisms, as required for an efficient oxidation of the plastoquinone pool. At first sight this seems to be a surprising finding given that there is a significant difference between the ground and excited states of the absorbing pigments. Yet, this does not necessarily translate into a decreased driving force for electron transfer, since the primary electron donor in *A. marina* could be a Chl *a* rather than a Chl *d*. Such a hypothesis would be in line with the combined proposals that (i) the primary electron donor in Chl *a* containing PSI is not the Chl *a* heterodimer of P_{700} but an accessory Chl *a* (ec2) monomer (43, 44) and (ii) in *A. marina* PSI, at least one of the two accessory Chls involved in charge separation has an absorption maximum ~680 nm, suggesting that it is a Chl *a* (45). It is of note, however, that Kumazaki *et al.* (45) assigned the bleaching they observed at 680 nm, which is formed and decays with time constants of ~6 and 50 ps, respectively, to the primary electron acceptor rather than to the primary electron donor as we consider here.

Clearly, the hypothesis that Chl *a* is involved in primary charge separation in PSI of *A. marina* would require a thermally activated transfer of the exciton between the light-harvesting Chl *d* and the photochemical trap. Although a hint pointing to such an activated excitonic transfer can be found in the ultrafast studies by Kumazaki *et al.* (45), who reported a rather slow exciton trapping time (~50 ps), the mere observation that PSI from *A. marina* is still photochemically active at 77 K (39) is at odds with a significant difference in energy level between the excited states of the primary electron donor and of the antenna Chls.

Thus, an alternative hypothesis would be that either the reducing power (*i.e.* the midpoint potential of the P^*/P^+ couple, where P denotes the primary electron donor without any assumption as to whether it is either one of the two P_{740} (ec1) or accessory (ec2) Chls) or the oxidizing power (*i.e.* the midpoint potential of the P/P^+ couple) is decreased.

In a survey of the available data on type I reaction centers from a variety of organisms, including *A. marina*, Itoh *et al.* (46) proposed that the reducing power of the acceptor side of type I reaction centers is conserved in all of the photosynthetic organisms (green sulfur bacteria, heliobacteria, and oxygenic organisms in general). According to these authors, the requirement for preserving the reducing power of the P* state, despite different transition energies between the ground and excited states of their primary Chl electron donors, stems from the necessity to optimize the primary and secondary electron transfer reactions. Thus, any change in the energy of the exciton that drives the primary photochemistry would require a compensatory change of the E_m of the primary electron donors to the reaction center in order to preserve this optimization.

This proposal is supported, at first sight, by both green sulfur bacteria and heliobacteria, in which the decreased E_m of the primary donor (the midpoint potential of the Chl dimer corresponding to P_{700} or P_{740}) is down-shifted by ~200 mV (for reviews, see Refs. 47 and 48), which matches the decrease in energy supply to PSI photochemistry (in the case of green sulfur bacteria, the absorbed photon is at ~800 nm; *i.e.* ~250 meV lower than for a 700 nm photon). However, the overall photosynthetic electron transfer chain from either of these strictly anaerobic photosynthetic bacteria differs from those from Chl

a and probably also from Chl *d* containing oxygenic phototrophs in several respects beyond the nature of the Chls involved in electron transfer. Indeed, the quinone serving as the electron donor to the cytochrome b_6f complex in these anaerobes is a menaquinone-9 and not a plastoquinone. The midpoint potential of the MKH_2/MK couple is more negative than that of the PQH_2/PQ couple, which acts as the electron carrier between PSII and the cyt b_6f complex in oxygenic photosynthetic chain. Although the available reducing power for electron transfer from the quinol is thus larger, it is remarkable that not only the midpoint potential of the P^+/P couple but also those of the cyt *c*, b_H, and b_L from the cyt b_6c complex are down-shifted in *H. mobilis* with respect to their homologous cofactors in oxygenic photosynthetic organisms (40, 47). Therefore, the driving force for the oxidation of MKH_2 at the Q_0 site, on the one hand, and for the electron transfer between the cyt b_6c cofactors and P^+, on the other hand, are preserved. In brief, in heliobacteria and green sulfur bacteria, the relatively large reducing power of the quinol is compatible with a shift of the midpoint potential of the P^+/P couple and the resulting conservation of the reducing power at the acceptor side of PSI.

Clearly, such a strategy is hardly conceivable in *A. marina*, where the energy gap between the plastoquinone (E_m ~+100 mV) and P_{740} (E_m ~+425 mV determined in this work) is only ~325 mV. The resulting relatively small energy gap might be expected to impose a major constraint to the electron flow process. However, any change in the E_m value of the cyt b_6f complex, required to keep a high driving force for electron flow to PSI, would certainly affect the driving force for PQH_2 oxidation and therefore decrease the efficiency of PSII-driven electron flow.

In actual fact, our current understanding of the energetic picture of PSI, as a photochemical energy converter, shows that it can accommodate a lower excitonic driving force without suffering a significant loss in its efficiency. In Chl *a*-containing PSI, according to recent data, the time constant and driving force of the primary radical pair (RP1) formation are 7 ps and 65 meV, respectively (43). This initially formed radical pair is composed of $Chl^+A_o^-$ ($ec2^+ec3^-$) (43, 44), which is further stabilized by the formation of the $P^+A_o^-$ ($ec1^+ec3^-$) (RP2) state with a time constant of 20 ps (43). From luminescence measurements, the free energy difference between the excited state RP* and RP2 was estimated to be ~250 meV (49, 50), suggesting that the free energy change associated with the formation of RP2 at the expense of RP1 is ~190 meV. Finally, the $P^+A_1^-$ ($ec1^+A_1^-$) state is formed at the expense of RP2 with a 30 ps time constant and a driving force of 340 meV. Therefore, charge separation is stabilized with a time constant of 30 ps and a free energy change of ~600 meV. Although substituting a Chl *d* for a Chl *a* in the charge transfer chain may render the formation of RP1 to be slightly uphill in energy (but see Ref. 51 for a different view), the overall photochemical efficiency of PSI should not be significantly altered, because this step is followed by two sequential steps that are strongly downhill in energy and fast enough to compete with charge recombination losses and allow the stabilization of the radical pair with a high quantum yield.

From the above considerations, it is not necessary to make the midpoint potential of the PSI electron acceptor the reference that would affect the electrochemical engineering of the entire photosynthetic chain. If indeed such a reference is needed, the midpoint potential of the PQ pool would, in our view, be more relevant for the following reasons: (i) the PQ pool interacts with two different membrane complexes, PSII and the cyt b_6f complex, and their electrochemical properties would have to be constrained in a concerted way; (ii) PQH_2 oxidation at the Qo site of the cyt b_6f complex is the rate-limiting step in the whole photosynthetic chain, so that the overall photosynthetic activity is expected to be quite sensitive to any change in the energetics of this oxidation reaction; (iii) the overall free energy change associated with the reduction of the terminal PSI electron acceptor $NADP^+$ (E_m ~−320 mV) by the formation of a long lived cation in PSI is about 750 meV. It is significantly larger than the free energy change of ~500 meV associated with the electron transfer between Q_A^-, the primary quinone electron acceptor in PSII, and the primary electron donor in PSI, especially because some of this free energy is used by the cyt b_6f complex to drive the Q-cycle. Accordingly, the lack of changes in the E_m of P_{740} and cyt *f* observed in *A. marina* on the one side and the down-shifted midpoint potential of the Chl dimer in type I reaction centers from heliobacteria and green sulfur bacteria can both be explained in terms of the stronger reducing power of menaquinol, with respect to plastoquinol, rather than by the lower excitonic load that drives the photosynthetic chain in these organisms.

Electron Flow Is Not Restrained by Diffusion-limiting Domains in A. marina—A corollary to our characterization of electron flow in *A. marina* is the finding that the experimentally determined equilibrium constant, K_{fp}-exp between cyt *f* and P_{740} nicely agrees with the theoretical one, K_{fp}-theor, expected from the midpoint potentials of these two cofactors. Although one would expect such an agreement to prevail, this is, to our knowledge, the first reported case where it is met and, as we will now briefly discuss, it may be a reflection of significant ultrastructural differences between the supramolecular organization of the photosynthetic chain in thylakoids from vascular plants and cyanobacteria.

The difference between K_{fp}-exp and K_{fp}-theor has been interpreted as reflecting the existence of plastocyanin (PC) diffusion domains, with different stoichiometries of PSI, PC, and cyt b_6f complexes. These domains have been tentatively suggested to be the different chloroplast compartments previously identified by Albertsson (52, 53), namely the grana stacks, the end and margin membranes, and the stroma lamellae. Within this structurally based model, the rationale for the discrepancy between K_{fp}-exp and K_{fp}-theor is the following. Due to uneven stoichiometry of the different membrane complexes, P_{700} can be photo-oxidized in the domains with a high P_{700}/(cyt *f* + PC) ratio, well before cyt *f* oxidation is fully completed in the other domains with a low P_{700}/(cyt *f* + PC) ratio. In this case, coexistence of cyt f^+ and P_{700}^+ is observed when the redox state of the two cofactors is probed simultaneously in all of the domains, resulting in the estimation of a low K_{fp}-exp (*e.g.* see Refs. 54–56 and also Ref. 57).

In the case of the *A. marina* cells used in the present study, the thylakoids do not show the presence of any grana and lamella domains (58). Thus, the good agreement between K_{fp}-

exp and K_{fp}-theor observed in this organism supports the hypothesis of a correlation between the presence of confined diffusion domains and the macroscopic differentiation of the thylakoid membranes in plants and green algae.

In such a homogeneous system, one could expect PSI and PSII to coexist in the same domains. However, the fluorescence induction curves in the presence of DCMU show both a high F_v/F_m and a sigmoidal shape, indicating that, on the one hand the probability for energy transfer between PSII units is significant and that on the other hand there is little excitonic transfer PSII to PSI. Altogether, these data suggest that PSII and PS1 are present in the same membrane domains but do not share their antenna, raising the issue of the segregation between the two PS types. Previous analysis of the cyanobacterium *Synechocystis* 6714 provides a structural answer to this question. Freeze-fracture pictures of thylakoid membranes frequently show rows of EF particles (*e.g.* see Ref. 59), which are attributed to an organized arrangement of PSII complexes in the membranes. Clearly, a similar situation may take place in *A. marina*, as suggested by the ultrastructural data, which show this photosystem to arranged as a dimer within a giant complex surrounded by light-harvesting Pcb proteins (60), a feature that may extend to even larger aggregates of PSII within the membrane (5), thereby accounting for the energetic segregation between PSI and PSII in an otherwise freely diffusing system.

Acknowledgments—We thank Sam Benson for cultivating cells of A. marina and Ghada Ajlani for skillful advice.

REFERENCES

1. Miyashita, H., Ikemoto, H., Kurano, N., Adachi, K., Chihara, M., and Miyachi, S. (1996) *Nature* **383,** 402
2. Kuhl, M., Chen, M., Ralph, P. J., Schreiber, U., and Larkum, A. W. (2005) *Nature* **433,** 820
3. Murakami, A., Miyashita, H., Iseki, M., Adachi, K., and Mimuro, M. (2004) *Science* **303,** 1633
4. Miller, S. R., Augustine, S., Olson, T. L., Blankenship, R. E., Selker, J., and Wood, A. M. (2005) *Proc. Natl. Acad. Sci. U. S. A.* **102,** 850–855
5. Marquardt, J., Senger, H., Miyashita, H., Miyachi, S., and Morschel, E. (1997) *FEBS Lett.* **410,** 428–432
6. Hu, Q., Marquardt, J., Iwasaki, I., Miyashita, H., Kurano, N., Morschel, E., and Miyachi, S. (1999) *Biochim. Biophys. Acta* **1412,** 250–261
7. Manning, W. M., and Strain, H. H. (1943) *J. Biol. Chem.* **151,** 1–19
8. Hu, Q., Miyashita, H., Iwasaki, I. I., Kurano, N., Miyachi, S., Iwaki, M., and Itoh, S. (1998) *Proc. Natl. Acad. Sci. U. S. A.* **95,** 13319–13323
9. Hurt, E. C., and Hauska, G. (1981) *Eur. J. Biochem.* **117,** 591–599
10. Kramer, D. M., and Crofts, A. R. (1994) *Biochim. Biophys. Acta* **1184,** 193–201
11. Pierre, Y., Breyton, C., Kramer, D., and Popot, J.-L. (1995) *J. Biol. Chem.* **49,** 29342–29349
12. Nakamura, A., Suzawa, T., Kato, Y., and Watanabe, T. (2005) *FEBS Lett.* **579,** 2273–2276
13. Witt, H., Bordignon, E., Carbonera, D., Dekker, J. P., Karapetyan, N., Teutloff, C., Webber, A., Lubitz, W., and Schlodder, E. (2003) *J. Biol. Chem.* **278,** 46760–46771
14. Keller, M. D., Selvin, R., Claus, W., and Guillard, R. R. L. (1987) *J. Phycol.* **23,** 633–638
15. Miyashita, H., Adachi, K., Kurano, N., Ikemoto, H., Chihara, M., and Miyachi, S. (1997) *Plant Cell Physiol.* **38,** 274–281
16. Aiba, H., Adhya, S., and de Crombrugghe, B. (1981) *J. Biol. Chem.* **256,** 11905–11910
17. Béal, D., Rappaport, F., and Joliot, P. (1999) *Rev. Sci. Instr.* **70,** 202–207
18. Li, Y., Lucas, M. G., Konovalova, T., Abbott, B., MacMillan, F., Petrenko, A., Sivakumar, V., Wang, R., Hastings, G., Gu, F., van Tol, J., Brunel, L. C., Timkovich, R., Rappaport, F., and Redding, K. (2004) *Biochemistry* **43,** 12634–12647
19. Alric, J., Pierre, Y., Picot, D., Lavergne, J., and Rappaport, F. (2005) *Proc. Natl. Acad. Sci. U. S. A.* **102,** 15860–15865
20. Schiller, H., Senger, H., Miyashita, H., Miyachi, S., and Dau, H. (1997) *FEBS Lett.* **410,** 433–436
21. Chen, M., Quinnell, R. G., and Larkum, A. W. (2002) *FEBS Lett.* **514,** 149–152
22. Boichenko, V. A., Klimov, V. V., Miyashita, H., and Miyachi, S. (2000) *Photosynth. Res.* **65,** 269–277
23. Delosme, R., Joliot, P., and Lavorel, J. (1959) *C. R. Acad. Sci. Paris* **249,** 1409–1411
24. Butler, W. L. (1978) *Annu. Rev. Plant Physiol.* **29,** 345–378
25. Genty, B., Briantais, J.-M., and Baker, N. R. (1989) *Biochim. Biophys. Acta* **990,** 87–92
26. Campbell, D., Hurry, V., Clarke, A. K., Gustafsson, P., and Oquist, G. (1998) *Microbiol. Mol. Biol. Rev.* **62,** 667–683
27. Biggins, J., and Bruce, D. (1989) *Photosynth. Res.* **20,** 1–34
28. Joliot, P., and Joliot, A. (1964) *C. R. Acad. Sci. Paris* **258,** 4622–4625
29. Lavergne, J., and Trissl, H.-W. (1995) *Biophys. J.* **65,** 2474–2492
30. Rappaport, F., Beal, D., Joliot, A., and Joliot, P. (2007) *Biochim. Biophys. Acta* **1767,** 56–65
31. Finazzi, G., Furia, A., Barbagallo, R. P., and Forti, G. (1999) *Biochim. Biophys. Acta* **1413,** 117–129
32. Trebst, A. (1980) *Methods Enzymol.* **69,** 675–715
33. Pettigrew, G. W., and Moore, G. R. (1987) *Cytochromes c: Biological Aspects* (Rich, A., ed) pp. 14–15, Springer-Verlag, Berlin
34. Witt, H. T. (1979) *Biochim. Biophys. Acta* **505,** 355–427
35. Baymann, F., Rappaport, F., Joliot, P., and Kallas, T. (2001) *Biochemistry* **40,** 10570–10577
36. Hope, A. B. (2000) *Biochim. Biophys. Acta* **1456,** 5–26
37. Swingley, W. D., Chen, M., Cheung, P. C., Conrad, A. L., Dejesa, L. C., Hao, J., Honchak, B. M., Karbach, L. E., Kurdoglu, A., Lahiri, S., Mastrian, S. D., Miyashita, H., Page, L., Ramakrishna, P., Satoh, S., Sattley, W. M., Shimada, Y., Taylor, H. L., Tomo, T., Tsuchiya, T., Wang, Z. T., Raymond, J., Mimuro, M., Blankenship, R. E., and Touchman, J. W. (2008) *Proc. Natl. Acad. Sci. U. S. A.* **105,** 2005–2010
38. Itoh, S., Mino, H., Itoh, K., Shigenaga, T., Uzumaki, T., and Iwaki, M. (2007) *Biochemistry* **46,** 12473–12481
39. Schlodder, E., Çetin, M., Eckert, H. J., Schmitt, F. J., Barber, J., and Telfer, A. (2007) *Biochim. Biophys. Acta* **1767,** 589–595
40. Kramer, D. M., Schoepp, B., Liebl, U., and Nitschke, W. (1997) *Biochemistry* **36,** 4203–4211
41. Schenderlein, M., Çetin, M., Schlodder, E., Benson, S., Sharma, P. K., Barber, J., and Telfer, A. (2007) in *14th International Congress on Photosynthesis Research* (Allen, J. F., ed) pp. 215–218, Kluwer Academic Publishers, Glasgow, UK
42. Tomo, T., Kato, Y., Suzuki, T., Akimoto, S., Okubo, T., Noguchi, T., Hasegawa, K., Tsuchiya, T., Tanaka, K., Fukuya, M., Dohmae, N., Watanabe, T., and Mimuro, M. (2008) *J. Biol. Chem.* **283,** 18198–18209
43. Holzwarth, A. R., Muller, M. G., Niklas, J., and Lubitz, W. (2006) *Biophys. J.* **90,** 552–565
44. Li, Y., van der Est, A., Lucas, M. G., Ramesh, V. M., Gu, F., Petrenko, A., Lin, S., Webber, A. N., Rappaport, F., and Redding, K. (2006) *Proc. Natl. Acad. Sci. U. S. A.* **103,** 2144–2149
45. Kumazaki, S., Abiko, K., Ikegami, I., Iwaki, M., and Itoh, S. (2002) *FEBS Lett.* **530,** 153–157
46. Itoh, S., Iwaki, M., and Ikegami, I. (2001) *Biochim. Biophys. Acta* **1507,** 115–138
47. Nitschke, W., Liebl, U., Matsuura, K., and Kramer, D. M. (1995) *Biochemistry* **34,** 11831–11839
48. Blankenship, R. E. (1992) *Photosynth. Res.* **33,** 91–111
49. Kleinherenbrink, F. A. M., Hastings, G., Wittmershaus, B. P., and Blankenship, R. E. (1994) *Biochemistry* **33,** 3096–3105
50. Vos, M. H., and van Gorkom, H. J. (1990) *Biophys. J.* **58,** 1547–1555
51. Kobayashi, M., Ohashi, S., Iwamoto, K., Shiraiwa, Y., Kato, Y., and Wa-

tanabe, T. (2007) *Biochim. Biophys. Acta* **1767,** 596–602
52. Albertsson, P.-Å. (1988) *Q. Rev. Biophys.* **21,** 61–98
53. Albertsson, P.-Å., Andreasson, E., Svensson, P., and Yu, S.-G. (1991) *Biochim. Biophys. Acta* **1098,** 90–94
54. Lavergne, J., and Joliot, P. (1991) *Trends Biochem. Sci.* **16,** 129–134
55. Joliot, P., Lavergne, J., and Beal, D. (1992) *Biochim. Biophys. Acta* **1101,** 1–12
56. Lavergne, J., Bouchaud, J. P., and Joliot, P. (1992) *Biochim. Biophys. Acta* **1101,** 13–22
57. Kirchhoff, H., Schottler, M. A., Maurer, J., and Weis, E. (2004) *Biochim. Biophys. Acta* **1659,** 63–72
58. Swingley, W. D., Hohmann-Marriott, M. F., Le Olson, T., and Blankenship, R. E. (2005) *Appl. Environ Microbiol.* **71,** 8606–8610
59. Olive, J., M'Bina, I., Vernotte, C., Astier, C., and Wollman, F.-A. (1986) *FEBS Lett.* **208,** 308–312
60. Chen, M., Bibby, T. S., Nield, J., Larkum, A. W., and Barber, J. (2005) *FEBS Lett.* **579,** 1306–1310